Crystal Nucleation and Growth in Large Clusters of SeF_6 from Molecular Dynamics Simulations

Yaroslav Chushak and Lawrence S. Bartell*

Department of Chemistry, University of Michigan, Ann Arbor, Michigan 48109

Received: June 12, 2000; In Final Form: August 9, 2000

An account of a computer simulation of the nucleation kinetics and crystal growth during the freezing of a series of SeF_6 clusters is presented. Although SeF_6 has a stable monoclinic phase at the temperatures studied, the clusters froze initially to the body-centered cubic phase and then transformed to the low-energy structure. The temperature dependence of the nucleation rate obtained in the simulations is in approximate agreement with that predicted by the classical nucleation theory. A theoretical model of cluster crystallization that includes time-dependent nucleation and finite-size effects is proposed, applied, and found to accord well with the molecular dynamics (MD) data. Three order parameter profiles, namely, density, translational order, and molecular orientational order, were calculated for nuclei close to the critical size. The orientational order parameter is a new one, presented here for the first time. The translational order parameter shows a weak temperature dependence, while the orientational order parameter for the solid significantly increases with the deepening of supercooling. It is found that the translational order parameter extends well beyond the radius at which the density falls to the liquid value. That is, the nucleus is a reasonably dense crystalline particle surrounded by a layer of molecules with a liquid density but possessing a translational periodicity. This result agrees with prior conclusions of density functional treatments and molecular dynamics simulations for monatomic systems. Order parameter profiles, then, offer several very different estimates of the sizes of critical nuclei. The estimate based on the density and orientational order is roughly in agreement with that predicted by the classical nucleation theory. The size based on translational order is much larger, perhaps by 6-fold, and agrees with our estimates based on fluctuations in sizes of bulklike embryos (identified by their translational order). Turnbull's hypothesis of negative excess interfacial entropy of the liquid in contact with the solid, together with the implied consequences if the larger nuclear size is accepted, suggests that the density profile offers the most realistic estimate of the size of critical nuclei.

Introduction

The crystallization of supercooled liquids has been a subject of investigation of scientists, both experimentalists and theorists, for many years. Despite this activity, our understanding of the mechanism of phase transformations on the microscopic level is still limited due to the complexity of the problem.[1,2] Existing theories require a knowledge of the thermodynamic and physical properties of supercooled materials that is not readily available, particularly at deep supercooling. On the other hand, molecular dynamics (MD) simulations give an exceptional opportunity, not only to deduce the required properties but also to monitor the motion of individual molecules and to follow their cooperative motions during the process of crystallization.[3]

Recently we presented the results of MD simulations of the spontaneous phase transformations during the freezing of two sets of clusters of selenium hexafluoride at 140 and 130 K.[4] The first set contained 12 clusters with 725 molecules of SeF_6, and the second set had 10 clusters with 1722 molecules. Although the stable phase of SeF_6 at the temperatures studied is monoclinic, clusters froze initially to the body-centered cubic (bcc) phase and then transformed to the low-energy structure. Such a two-stage crystallization with a formation of a metastable phase is a common process for a wide variety of materials ranging from metals to polymers.[5] The aim of the present paper is to analyze the kinetics of nucleation and growth during the crystallization of SeF_6 clusters.

Crystal nucleation in molecular clusters involves changes in the average particle density, translational periodic structure, and orientational order of molecules, each of which can be taken as an order parameter. This is not to imply that all three order parameters go together during the phase transformation. The analysis of order parameter profiles for a monatomic system, in treatments via both density functional theory[6] and molecular dynamics simulations,[7] shows that the density order profile decays faster than the structural order, i.e., that the solidlike core is surrounded by a shell of atoms with nearly liquid density but with strong vestiges of solidlike order. However, to the best of our knowledge, nothing has been published about the behavior of the orientational order parameter. The present study is the first step in this direction.

It is known that the crystallization of supercooled liquids is an activated process which occurs by crystal nucleation and growth. The evolution of phase transformations, occurring by nucleation and growth processes, is usually represented by the Johnson−Mehl−Avrami−Kolmogorov (JMAK) equation.[8−10] The original version of JMAK theory was developed for systems of infinite dimensions. Only recently was this theory extended for finite systems.[11−13] We have analyzed the kinetics of the two-stage crystallization of SeF_6 clusters adopting the model proposed by Kelton et al.,[13] which allows us to estimate the growth rates for liquid−bcc phase transformation.

10.1021/jp002107e CCC: $19.00
Published on Web 09/19/2000

Summary of Simulations

To set the stage for the present investigation, we briefly sketch the results of the computer simulations of the freezing of selenium hexafluoride clusters presented in detail in our previous paper.[4] Molecular dynamics simulations were performed on clusters containing 881 and 2085 molecules of SeF_6, which were taken to be rigid octahedra. Simulations were carried out at constant temperature using a seven-site intermolecular interaction function.[14] For both cluster sizes, an initial, approximately spherical cluster was constructed to be in its low-temperature monoclinic phase. During heating from 100 to 260 K, clusters transformed from the monoclinic to the body-centered cubic phase at about 150 K (881 molecules) or at 155 K (2085 molecules) and melted at 200 or 210 K, respectively.

The final configuration at 230 K was additionally equilibrated to generate 12 saved configurations for an 881-molecule cluster and 10 saved configurations for a 2085-molecule cluster to serve as independent starting configurations for cooling runs. During the heating and equilibration at 230 K, some of the molecules evaporated from the clusters and final configurations contained different numbers of liquid molecules. Therefore, to make the members of the set equivalent, approximately spherical configurations were constructed by trimming down clusters to a size of 725 molecules (smaller cluster) or 1722 molecules (larger cluster). Production runs for crystallization were carried out at 140 and 130 K for both sets of clusters and additionally at 100 K for the 725-molecule clusters.

During the nanosecond runs of the simulations, all of these clusters froze initially to the bcc structure characterized (as in the bulk crystals) by a large disorder in molecular orientations.[15] At the higher temperature, all but one of the larger clusters underwent a transition to the low-energy, ordered monoclinic structure whereas all but one of the smaller clusters remained bcc. At the lower temperature all of the smaller clusters ultimately transformed, usually quite abruptly, to the monoclinic structure. In the case of the larger clusters, a transition to the monoclinic phase was observed at 140 K whereas, at 130 K, besides the monoclinic structure, an orthorhombic phase, or a mixture of orthorhombic and monoclinic phases, was obtained in a few clusters. In both cases, the solid-state transition to the low-energy phase usually occurred when the number of bcc molecules had reached its maximum. Many of the larger frozen clusters were polycrystalline while the smaller ones were single crystals. A striking result of our simulations was that nucleation almost always occurred at or near the clusters' surfaces despite the fact that surfaces of clusters tend to be more disordered and melt at significantly lower temperatures than their cores. Phase transitions were recognized from the evolution of configurational energy and from the structure analyses described in the next section.

Structure Analyses

Identification of Phases. Several criteria can be used to identify the crystalline structure in molecular dynamics simulations. The most widely used technique to distinguish between molecules in liquid and in solid environments (used also in our previous study) is the very sensitive analysis of Voronoi polyhedra.[16] A Voronoi polyhedron for a given molecule is defined as a set of all points in space that are closer to that molecule than to any of the others. Since the surface molecules have an open space and may not be encompassed by complete polyhedra, they are neglected in such analyses. In the present study, we preferred the bond-order parameter method[17−19] to analyze molecular environments because it allows us to take surface molecules into consideration as well. Furthermore, this technique is suitable for discriminating not only between liquid and solid molecules but also between molecules in bcc and in monoclinic phases. Voronoi polyhedra fail to do that.

Translational Order. To recognize translational order or the degree of crystallinity in the case of liquid−solid transitions, we define "bonds" in terms of unit vectors $\mathbf{r}_{ij}$ joining the center of mass of molecule i with the center of mass of the neighbor molecules j that are within a given radius r_{cut} of i. Such "bonds," of course, do not correspond to those of conventional chemical usage. The orientation of the bond $\mathbf{r}_{ij}$ with respect to some reference coordinate system is specified by the spherical harmonics $Y_{lm}(\mathbf{r}_{ij}) = Y_{lm}(\theta_{ij};\varphi_{ij})$, where θ_{ij} and φ_{ij} are the polar and azimuthal angles of vector $\mathbf{r}_{ij}$ in this reference frame. Only even-l spherical harmonics, which are invariant under inversion, are considered. The local order around the molecule i is calculated by averaging over all bonds with its neighbors $N_{nb}(i)$:[19]

$$q_{lm}^{tr}(i) = \frac{1}{N_{nb}(i)} \sum_{j=1}^{N_{nb}(i)} Y_{lm}(\mathbf{r}_{ij}) \tag{1}$$

To avoid the dependence of the local order parameter on the choice of reference system, second-order invariants can be constructed:

$$q_l^{tr}(i) = \left(\frac{4\pi}{2l+1} \sum_{m=-l}^{l} |q_{lm}^{tr}(i)|^2 \right)^{1/2} \tag{2}$$

The global order parameter Q_l^{tr} can be obtained by averaging $q_{lm}^{tr}(i)$ over all N molecules in a cluster:

$$Q_{lm}^{tr} = \left(\frac{4\pi}{2l+1} \sum_{m=-l}^{l} |\bar{Q}_{lm}^{tr}|^2 \right)^{1/2} \tag{3}$$

where

$$\bar{Q}_{lm}^{tr} = \frac{\sum_{i=1}^{N} N_{nb}(i) q_{lm}^{tr}(i)}{\sum_{i=1}^{N} N_{nb}(i)} \tag{4}$$

In an isotropic liquid state, the global bond-order parameter goes to zero in the thermodynamic limit for all values of $l > 0$. In a crystal, the bond orientations are correlated throughout the solid and the (nonvanishing) value of the order parameter Q_l^{tr} depends on the crystalline structure. For symmetry reasons, the first nonzero averages (other than the constant value for $l = 0$) occur at $l = 4$ in crystals with cubic symmetry and at $l = 6$ in aggregates with icosahedral symmetry. Therefore, we restrict ourselves to $l = 6$, an index which enables us to distinguish various solid structures from each other and from the liquid.

To identify a molecule as being in a solid or liquid state, we use a normalized $(2 \times 6 + 1)$-dimensional vector $\tilde{\mathbf{q}}_6^{tr}(i)$, with components[19]

$$\tilde{\mathbf{q}}_{6m}^{tr}(i) = \frac{q_{6m}^{tr}(i)}{\left[\sum_{m=-6}^{6} |q_{6m}^{tr}(i)|^2 \right]^{1/2}} \tag{5}$$

and a dot product of the vectors $\tilde{\mathbf{q}}_6^{\mathrm{tr}}$ of neighboring molecules *i* and *j*, defined as

$$\tilde{\mathbf{q}}_6^{\mathrm{tr}}(i)\,\tilde{\mathbf{q}}_6^{\mathrm{tr}}(j) \equiv \sum_{m=-6}^{6} \tilde{q}_{6m}^{\mathrm{tr}}(i)\,\tilde{q}_{6m}^{\mathrm{tr}}(j)^* \tag{6}$$

By construction, $\tilde{\mathbf{q}}_6^{\mathrm{tr}}(i)\,\tilde{\mathbf{q}}_6^{\mathrm{tr}}(i) = 1$. The molecules *i* and *j* are called "coherent" if the dot product $\tilde{\mathbf{q}}_6^{tr}(i)\,\tilde{\mathbf{q}}_6^{tr}(j)$ exceeds 0.5. Then, the molecule is identified as being solidlike if it is coherent with more than 70% of its neighbors. Thus, core molecules which have 14 neighbors should be coherent with at least 10 of their neighbors to be classified as solid. We also define as "bulklike" solid molecules as those solid molecules which are surrounded by at least 12 solid neighbors. These bulklike embryos that materialize and vanish as embryos are envisaged in the classical nucleation theory (CNT). Before nucleation occurs, however, there may be many contiguous molecules in thin sheets and filaments satisfying the solid but not the bulklike criterion for crystallinity, many more, in fact, than are believed to be in a critical nucleus. The concerted growth of nuclei signaling onset of nucleation always begins, however, with the appearance of bulklike aggregates.[4]

Orientational Order. Local orientational order parameters $q_{lm}^{\mathrm{or}}(i)$ of the octahedral molecules are based on the *chemical* bonds $\mathbf{r}_{in}^{\mathrm{ch}}$ joining the Se atom in the center of *i*th octahedra with the *n*th F atom in its vertex. We define this order parameter to be

$$q_{lm}^{\mathrm{or}}(i) = \frac{1}{6}\sum_{n=1}^{6} Y_{lm}(\mathbf{r}_{in}^{\mathrm{ch}}) \tag{7}$$

a quantity the same for all molecules independently of whether they are in the liquid or solid state. We adopt a dot product $\tilde{\mathbf{q}}_6^{\mathrm{or}}(i)\,\tilde{\mathbf{q}}_6^{\mathrm{or}}(j)$ to characterize the molecular orientational order in clusters and require it to be at least 0.5 for the *ij* pair to be "coherent." In the plastically crystalline bcc phase, the orientation of molecule *i* tends to be incoherent with the orientations of its neighbors *j*, and the dot product $\tilde{\mathbf{q}}_6^{\mathrm{or}}(i)\,\tilde{\mathbf{q}}_6^{\mathrm{or}}(j)$ is small. Therefore, if the orientation of a given molecule is coherent with the orientations of at least 50% of its neighbors, such a molecule is identified as being in the monoclinic phase (which is not plastically crystalline).

Cluster-Size-Dependent Crystallization Kinetics. The volume fraction of a parent phase, transformed isothermally into a new phase at a given time *t*, can be presented by the Johnson−Mehl−Avrami−Kolmogorov equation:

$$X(t) = 1 - \exp\{-X_{\mathrm{e}}(t)\} \tag{8}$$

where the extended volume fraction transformed $X_e(t)$ is given by

$$X_e(t) = \int_0^t J(t')\left[\int_{t'}^t \nu(\tau - t')\,\mathrm{d}\tau\right]\mathrm{d}t' \tag{9}$$

The extended volume $\nu(t)$ in eq 9 depends on the growth model considered. The standard version of JMAK theory was developed for an infinite system with the assumption that the size of the transformed regions is small compared with the sample size. Several attempts have been made to include finite-size effects in the analysis of the phase transformation kinetics.[11−13] In the present analysis we will follow the assumptions proposed by Kelton et al.[13] that are the most suitable for our case.

Let us consider the growth of a spherical nucleus with a radius *r* and a center at some random position *s* within a spherical cluster of radius *R* (Figure 1). The transformed volume at time *t* is given by

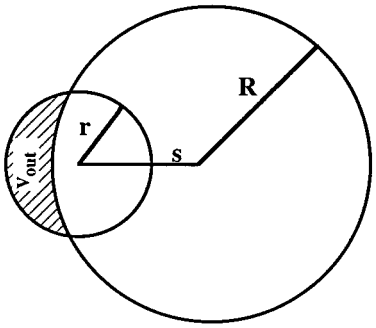

Figure 1. Representation of coordinates used in a model of crystal growth with the nucleation site located near the cluster's surface.

$$V_t = \frac{4}{3}\pi r^3 - V_{\mathrm{out}} \tag{10}$$

where

$$V_{\mathrm{out}} = \frac{\pi}{3}[(r-c)^2(2r+c) - (R-s-c)^2(2R+s+c)]$$

with

$$c = (R^2 - r^2 - s^2)/2s \tag{11}$$

For a system composed of a large number of spherical clusters of radius *R*, the average volume transformed $\nu(t)$ can be obtained by multiplying eq 10 by a weighting factor s^2 and integrating over the all possible locations of the growing nuclei in the cluster $s = [0, ..., R]$. The result obtained is[13]

$$\nu(t) = \frac{4}{3}\pi R^3\left(r^3 - \frac{9}{16}r^4 + \frac{1}{32}r^6\right) \tag{12}$$

where $r = Gt/R$ and *G* is the growth rate. Transformation is completed when $r = 2$. Although the weighting factor adopted does not include the preferential site dependence for nucleation found in our simulations, this neglect does not seem to greatly alter the integrated form of the growth kinetics.

Several approximations have been proposed in order to include into the JMAK theory the time dependence of the nucleation rate and the growth rate due to non-steady-state effects.[20−22] The simplest possible approximation is the form of a step function[23]

$$J(t) = \begin{cases} 0 & 0 \le t \le \tau \\ J_0 & \tau \le t \end{cases} \tag{13}$$

where J_0 is the steady-state nucleation rate and τ is the transient time. By inserting eqs 12 and 13 into eq 9, we obtained an expression that can be used as a first approximation to describe transient crystallization kinetics in supercooled clusters.

$$X(t) = 1 - \exp\left[-\pi J_0 G^3\left(\frac{(t-\tau)^4}{3} - \frac{3}{20}\frac{G}{R}(t-\tau)^5 + \frac{1}{168}\left(\frac{G}{R}\right)^3(t-\tau)^7\right)\right] \tag{14}$$

The crystallization of selenium hexafluoride clusters to the low-energy monoclinic phase can be considered a two-stage process: the liquid−solid transition to the metastable bcc phase with the nucleation rate J^{bcc}, transient time τ^{bcc}, and growth rate G^{bcc} and the solid-state transition to the stable monoclinic phase

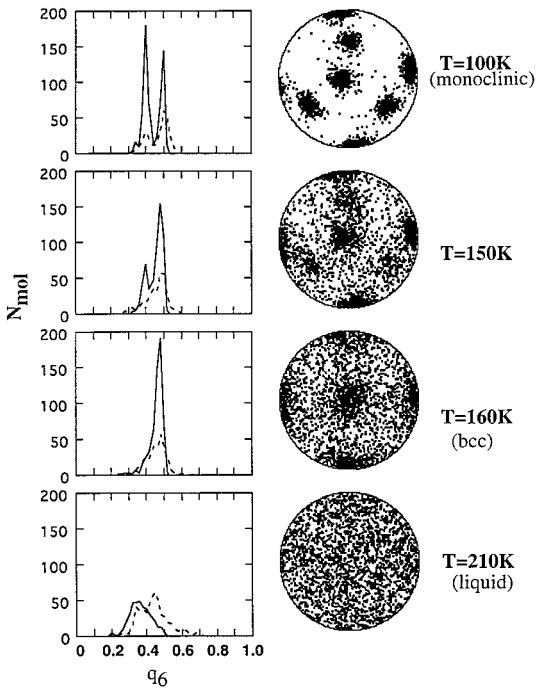

Figure 2. Distributions of the local order parameter $\mathbf{q}_6(i)$ together with Pawley projections of molecular bonds in the 881-molecule cluster at different temperatures during heating stages. Solid curves of $\mathbf{q}_6(i)$ correspond to bulk molecules and dashed lines correspond to surface molecules.

with the kinetic parameters J^{mono}, τ^{mono}, and G^{mono}. Such a two-stage process is in accord with Ostwald's "step rule", which posits for supercooled phase transitions that the first phase encountered is not the most stable phase but that with the closest free energy to the initial phase.[24] Only recently was the first attempt made to extend the JMAK theory to a two-stage crystallization process.[5] In the case of a cluster's two-stage crystallization, the volume fraction transformed to the stable phase is described by eq 14 with an explicit dependence on the radius of the metastable bcc crystallite $R(t)$.

Using reaction rate theory to calculate the net rate at which atoms are added to a nucleus of a given size, Kelton and Greer deduced that the average size-dependent growth rate is[25]

$$G(R) = \frac{16D}{\Delta r^2}\left(\frac{3V_m}{4\pi}\right)^{1/3} \sinh\left[\frac{V_m}{2k_B T}\left(\Delta G_v - \frac{2\sigma_{sl}}{R}\right)\right] \quad (15)$$

where D is the coefficient of diffusion in the supercooled liquid, V_m is the volume per molecule in the bcc phase, ΔG_v is the free-energy decrease per unit volume, Δr is the molecular jump distance taken to be $V_m^{1/3}$, and σ_{sl} is the interfacial energy per unit area.

Results

Characteristics of Phases. As mentioned in the foregoing, the bcc phase of selenium hexafluoride is plastically crystalline by virtue of a large disorder in molecular orientations. This disorder is a consequence of "orientational frustration" arising from the reluctance of the Se−F bonds with their negatively charged fluorines of neighboring molecules to point directly toward each other as they would in a "perfect" bcc crystal. The more ordered monoclinic phase differs from its bcc counterpart by a 60° rotation of one-third of the molecules which leads to a more efficient packing of fluorines.[15,26] Figure 2 shows the

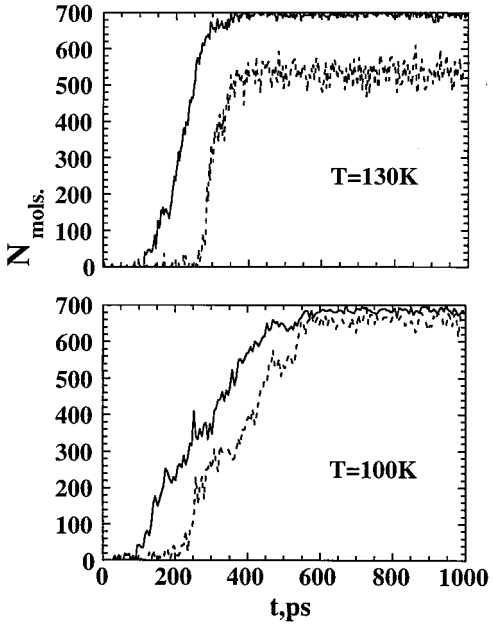

Figure 3. Typical time evolutions of a number of bulklike solid molecules (solid lines) and monoclinic molecules (dashed lines) for the 725-molecule clusters during the freezing at 130 K and 100 K.

distributions of the local order parameter $q_6^{tr}(i)$ together with the Pawley projections[27] (illustrating the projections of Se−F bond directions on a hemisphere over a cluster) corresponding to an 881-molecule cluster of SeF_6 as function of temperature during the heating process. In the low-temperature monoclinic phase, molecules have two different values of $q_6^{tr}(i)$ and two sets of three-spot patches that correspond to the two nonequivalent orientations of molecules in a unit cell. Surface molecules, defined as molecules that have less than 12 neighbors, display a broader distribution of the local order parameter due to their more irregular local structure (dashed curves in Figure 2). As the temperature warms to the monoclinic−bcc phase transition, the orientations of molecules become more disordered and the number of molecules with the lower value of $q_6^{tr}(i)$ decreases. In the bcc phase all molecules have the same translational order parameter and only exhibit one set of diffuse three-spot patches in the Pawley projection. The isotropic liquid structure is characterized by a wide distribution of $q_6^{tr}(i)$ as well as by completely disordered orientations of molecules.

Figure 3 presents the time evolution of the number of contiguous bulklike solid bcc and monoclinic molecules in a typical 725-molecule cluster during freezing at 130 and 100 K. At 130 K, transitions to the monoclinic phase usually began when the number of bcc molecules had reached its maximum. Because crystallization requires a major molecular translational reorganization, it is comparatively slow, usually taking 200−300 ps to complete. On the other hand, the solid-state transition from the bcc to the monoclinic phase involves only molecular reorientations and therefore takes only about 30 ps. At 100 K the transition to the low-energy phase began well before the freezing to bcc was complete. After the onset of formation of the monoclinic phase, the two phase transformations progressed simultaneously.

Critical Nuclei and Order Parameters. We have analyzed a number of configurations generated as discussed above to investigate the structure of critical nuclei during the liquid−solid transformation. Visual inspection shows that nuclei usually are formed near the surface of clusters. Although it is not straightforward to identify a critical nucleus, we subjectively

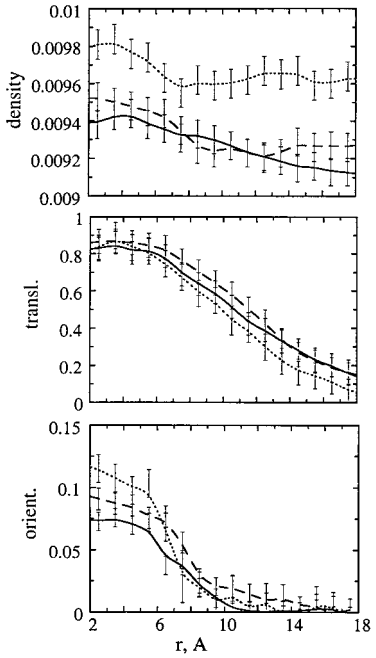

Figure 4. The density order, translational order, and molecular orientational order parameter profiles of the critical nucleus for the 725-molecule cluster at different temperatures, averaged over 12 independent cluster configurations.

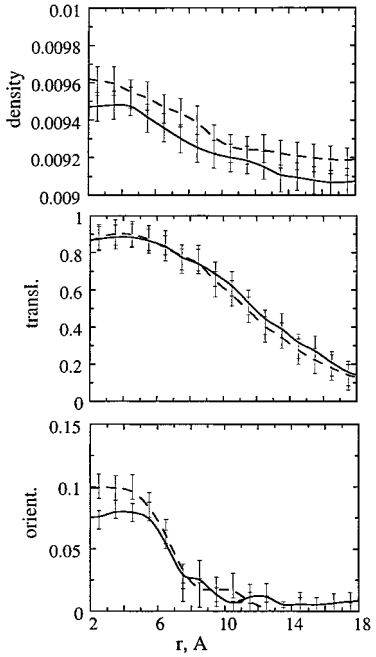

Figure 5. Same as in Figure 3 but for the 1722-molecule cluster. These data are averaged over 10 independent cluster configurations.

estimated the critical size from an examination of the fluctuations of embyros leading to the onset of crystal growth. It appeared that critical nuclei contain perhaps 25−30 molecules at 100 K, 45−50 molecules at 130 K, and 55−60 molecules at 140 K. Three order parameter profiles were calculated for critical nuclei: density, translational order, and molecular orientational order. While the first two order parameters have been studied theoretically as well as in MD simulations for monatomic systems, the orientational order parameter is a new one and, of course, one applicable only to molecular systems.

The density profiles were obtained by using the calculated volumes of Voronoi polyhedra. Because Voronoi polyhedra cannot be constructed around the surface molecules, they were excluded from the density profile calculations. For the translational and orientational order parameter profiles, a reference bond-orientation vector $\tilde{\mathbf{q}}_6^{\mathrm{od}}(\mathrm{ref})$ was calculated (od means tr or or) as a sum of vectors $\tilde{\mathbf{q}}_6^{\mathrm{od}}(i)$ over all molecules i in the critical nucleus. The value of the order parameter at a distance r from the center of the nucleus was calculated as a sum over the molecules j belonging to the corresponding shell.

$$od(r) = \sum_j \tilde{\mathbf{q}}^{od}(\mathrm{ref}) \cdot \tilde{\mathbf{q}}^{od}(j) \qquad (16)$$

Order parameter profiles for nuclei considered to be critical at different temperatures are presented in Figures 4 and 5 for 725- and 1722-molecule clusters, respectively.

Analyses of Nucleation Rate. The nucleation rate J is derived from the fraction of unfrozen clusters N_n/N_0 at time t_n that obeys the model first-order rate law

$$N_n/N_0 = \mathrm{e}^{-JV_c(t_n - t_0)} \qquad (17)$$

where N_0 is the number of clusters, V_c is the volume of the cluster, and t_0 is the time lag (a time when the first nucleation event has taken place, here assumed to be constant at a given temperature). Since the time t_n is that at which the nth nucleation event has occurred, N_n is taken to be[28]

$$N_n = N_0 - n + 1 \qquad (18)$$

From the slope of the plot $\ln(N_n/N_0)$ vs the time t_n, the quantity JV_c is obtained, and from the intercept, the time lag t_0 is obtained. Nucleation times t_n for freezing as well as for the solid-state bcc−monoclinic transitions can be readily recognized from the plots such as illustrated in Figure 3, but it is not clear what the time origin is for the solid-state nucleation time. Therefore, nucleation rates were estimated directly from MD simulations only for the liquid−solid phase transitions. Nucleation times for the crystallization of SeF_6 clusters together with the volumes per molecule V_c and the diffusion coefficients, used in the analysis of the nucleation rates, are listed in Tables 1 and 2.

TABLE 1: Nucleation Times for Freezing, Volumes Per Molecule, and Translation Diffusion Coefficients for the 725-Molecule Clusters

run no.	100 K	130 K	140 K
	t, ps		
1	240	140	265
2	347	165	620
3	115	210	260
4	450	215	230
5	220	120	150
6	215	225	250
7	315	200	210
8	150	60	80
9	120	175	280
10	285	155	415
11	125	140	490
12	120	190	300
	volume per molecule (Å^3)		
	104.0	108.6	109.8
	transl. diff. D (10^{-9} m ^{2}s^{-1})		
	0.16	0.48	0.70

In the theory of homogeneous nucleation, the nucleation rate is expressed as

$$J = A \exp(-\Delta G^*/k_B T) \qquad (19)$$

TABLE 2: Nucleation Times for Freezing, Volumes Per Molecule, and Translation Diffusion Coefficients for the 1722-Molecule Clusters

run no.	130 K	140 K
	t, ps	
1	130	155
2	105	125
3	180	80
4	140	175
5	140	155
6	235	175
7	180	130
8	120	85
9	200	290
10	126	165
	volume per molecule (Å^3)	
	108.6	110.0
	transl. diff. D (10^{-9} m ^{2}s^{-1})	
	0.4	0.55

where A is a prefactor and ΔG^* is the free energy of formation of a critical nucleus of the crystalline phase. The expressions for the nucleation and growth rates originate from the same set of coupled differential equations and usually contain the same set of kinetic parameters. A variant of the prefactor given by

$$A = 16\left(\frac{3\pi}{4}\right)^{1/3}\left(\frac{\sigma_{sl}}{k_B T}\right)^{1/2}\frac{D}{V_m^{2/3}\Delta r^2} \tag{20}$$

and based on viscous flow in the liquid to model the molecular jump across the solid−liquid interface[29] was adopted. Two different formulations for the free energy barrier ΔG^* were applied to analyze the temperature dependence of the nucleation rate. One is the classical (capillary) nucleation theory developed by Turnbull and colleagues.[30,31] Within the CNT, the expression for ΔG^* that takes into account the effect of Laplace pressure can be written as[32]

$$\Delta G^* = 16\pi\sigma_{sl}^3/[3(\Delta G_v + w')^2] \tag{21}$$

where w' arises from the change in free energy accompanying a change in the surface area of the freezing cluster, radius R, during nucleation, and given by

$$w' = P_L(\rho_l - \rho_s)/\rho_l$$

with P_L representing the Laplace pressure $2\sigma_l/R$ inside the cluster and the ρ's representing densities. The unknown quantity in eqs 20 and 21, and therefore the quantity derived from the nucleation rate, is the kinetic parameter σ_{sl} supposed to represent the interfacial free energy per unit area for the liquid−solid boundary. Another approach for the free energy of formation of a critical nucleus requiring the same input information is Gránásy's diffuse interface theory (DIT),[33] which explicitly take into account a thickness parameter for the interface between the two phases. The DIT expression for ΔG^*, including the correction for the effect of Laplace pressure, is given by[33,28]

$$\Delta G^* = -4\pi\delta^3\Delta G_v\psi/3 \tag{22}$$

with

$$\psi + [2(1+q)h^{-2} - (3+2q)h^{-1} + 1]/\eta$$

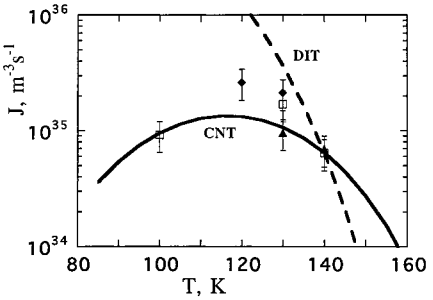

Figure 6. Temperature dependence of nucleation rate for the crystallization of SeF_6 clusters: solid triangles, 1722 molecule cluster; open squares, 725 molecule cluster; solid diamonds, 138 molecule cluster; solid line, classical nucleation theory (CNT); dashed line, diffuse interface theory (DIT).

where

$$\zeta = w/\Delta G_v \qquad \eta = \Delta G_{fus}/\Delta H_{fus}$$

$$h = \eta(1+\zeta) \qquad q = (1-h)^{1/2}$$

The unknown parameter in eq 22 is δ , considered to express the distance between the dividing surfaces for enthalpy and for entropy in the interface between the liquid and solid phases.

In Figure 6 we present the nucleation rate for different sizes of SeF_6 clusters as a function of temperature in comparison with the results of the CNT and DIT theoretical expressions. Following Gránásy, we took the CNT interfacial free energy σ_{sl} and the DIT distance δ to be independent of temperature for the purposes of the figure. These two parameters were estimated by adjusting them, via eqs 21 and 22, to reproduce the nucleation rate obtained from MD simulations at 140 K. Values so determined were $\sigma_{sl} = 0.013$ J/m^2 and $\delta = 1.56$ Å.

Kinetics of Crystal Growth. Records of the crystal growth for SeF_6 clusters obtained from MD simulations are presented in Figures 7 and 8 where they are compared with the results of theoretical calculations. MD curves (solid lines) are averaged over 12 independent configurations for the 725-molecule cluster and over 10 configurations for the 1722-molecule case. The temperature dependence of the growth rate obtained (see Table 3) agrees well with the results of the Kelton−Greer theory (eq 15). We present the growth rate vs nucleation rate for the bcc−monoclinic transition that correctly reproduces solid-state transformation kinetics in Figure 9.

Discussion

Temperature Dependence of Nucleation Rate. In general, the agreement between the CNT and MD data observed for the nucleation rates is quite good while that for the DIT is apparently not. The latter discrepancy, however, hinges about a single MD point obtained at such a deep supercooling that the solid-state transition started almost immediately after the onset of freezing, a behavior not characteristic of events represented by the other points. If this single point were discarded, the DIT would appear to account for the data more faithfully than the CNT. It is our subjective feeling that the DIT is at least as realistic as the CNT.

To examine the dependence of the nucleation rate on the size of clusters, we included the nucleation rates from our earlier study of 138-molecule clusters[28] in Figure 6 (solid diamonds). Uncertainties in the nucleation rates due to statistical uncertainties when the number of events is small prevent an accurate determination of the size effect, but one can perceive a tendency of the nucleation rate to increase as cluster sizes decrease. Several factors can lead to such a correlation. The most obvious

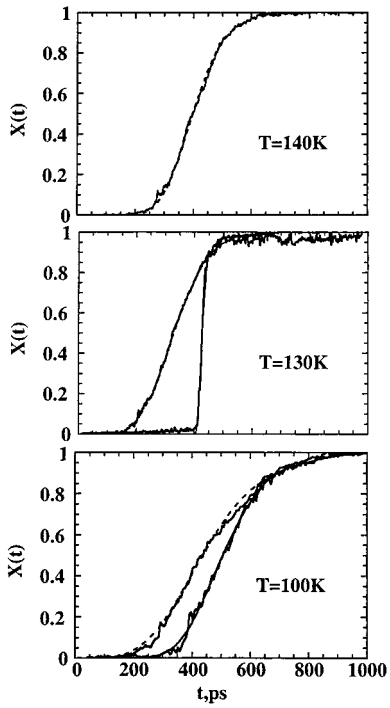

Figure 7. Volume fraction transformed as function of time for the 725-molecule cluster from MD simulations averaged over 12 independent clusters (solid lines) in comparison with the proposed model (dashed curves) at different temperatures.

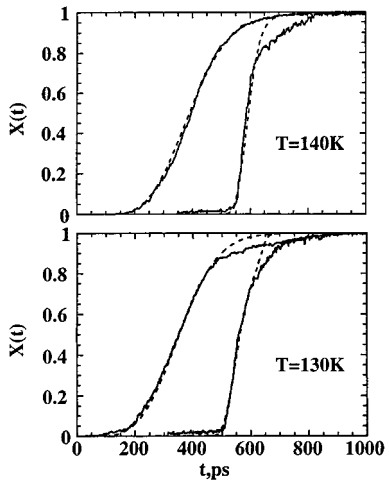

Figure 8. Same as in Figure 7 but for the 1722-molecule cluster. MD data are averaged over 10 independent cluster configurations.

is the effect of Laplace pressure that increases as the reciprocal of the cluster radius. Another factor which may affect the nucleation rate is the diffusion constant D, which is higher in the smaller cluster due to the relatively larger number of surface molecules of higher mobility. Finally, and perhaps most important, a visual analysis of crystallization shows that nuclei preferentially form at or near the cluster surface and not in the interior. Since smaller clusters have a higher surface/volume ratio, they have a higher number of preferred nucleation sites per unit volume.

Nucleation and Growth Rates. The phase transformation kinetics are governed by two material parameters: the nucleation rate J and the growth rate G. Within the theoretical model described above, we can reproduce the MD transformation curves by using a set of values of J and G. Therefore, there is some arbitrariness in the selection of these constants because we have to fix one of them. In the analysis of cluster

TABLE 3: Nucleation and Growth Rates for the SeF_6 Clusters

	nucleation rate (10^{35} m^{-3}s^{-1})		growth rate (m s^{-1})	
temp (K)	MD	model[a]	model	Kelton
		725 molecules		
140	0.64	1.7	12.5	11.6
130	2.2	2.2	10.	10.3
100	0.92	0.92	8.	8.1
		1722 molecules		
140	0.70	0.7	12.5	10.0
130	0.96	0.97	10.	9.3

[a] Selected to be compatible with MD nucleation rate. Once this rate is adopted, the model growth rate is fixed. Why the data for the 725-molecule cluster at 140 K is out of line with the other results is unclear.

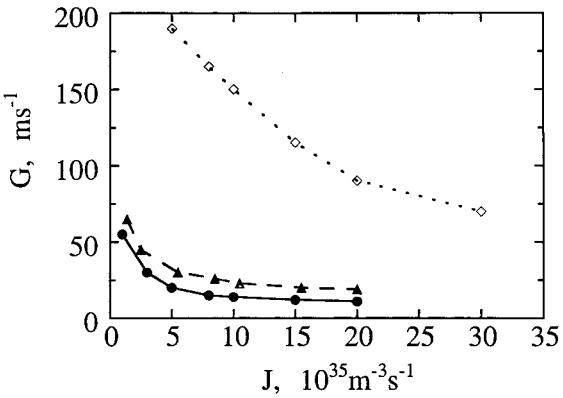

Figure 9. Sets of kinetic parameters (growth rate G vs nucleation rate J) that correctly reproduce the kinetics of bcc−monoclinic phase transformations; solid triangles, 1722 molecule cluster at $T = 140$ K; solid circles, the same cluster at $T = 130$ K; open diamonds, 725 molecule cluster at $T = 130$ K.

crystallization kinetics, the nucleation rates were chosen to be the same as those of the MD results, except for the smaller cluster at 140 K. The reason is that we could not obtain the correct transformation kinetics within the proposed model using the MD nucleation rate. It seems that this nucleation rate is too small due to statistical uncertainties. Furthermore, it is smaller than the nucleation rate for the larger cluster at the same temperature that contradicts the observed size effects on nucleation rates.

An excellent agreement between the MD simulations and the theoretical description of crystallization kinetics (eq 14) is obtained for the smaller cluster while, for the larger cluster, some discrepancies are observed at the final stage of crystal growth (Figures 7 and 8). Two sources may account for such a disagreement. (1) As reported previously,[4] the crystallization of 1722-molecule clusters is a polynuclear process where several nuclei grow simultaneously while crystallization for the smaller cluster is mononuclear. As a result, the final structure for the larger cluster is polycrystalline. The present method of identifying solidlike molecules does not consider molecules to belong to crystalline aggregates if they reside in somewhat disordered regions such as those occurring in the grain boundaries. (2) The theoretical model, itself, may not be correct in the case of polycrystalline growth.

In Table 3 we list the kinetic parameters obtained from the fitting of the solid−liquid growth curves of the MD simulations by the theoretical model. The temperature dependence of the growth rate is in good agreement with the results of Kelton−Greer theory (eq 15), which takes into account the size of a

cluster. On the other hand, we were unable to derive the nucleation rate for the bcc−monoclinic transformation from the MD simulations or to calculate the growth rate due to the lack of required information about the physical properties of SeF_6 at the solid−solid transition temperature. We present in Figure 9 a comparison of the growth rates that would account for the MD results of the bcc−monoclinic transition if the nucleaiton rates were known. The growth rate for the 725-molecule cluster exceeds, by several-fold, the growth rate for the larger cluster. This difference may be due to the fact that the liquid−bcc transition for the smaller cluster occurs from a single nucleus and attains an almost perfect bcc configuration before the bcc−monoclinic transition begins. In the case of the larger cluster, the liquid−solid transition is a polynuclear process and the final bcc configuration is polycrystalline with many defects in the grain boundaries. These irregularities, associated with the different spatial orientations of the crystallites, may retard the bcc−monoclinic growth.

Order Parameters and Sizes of Critical Nuclei. At all temperatures studied, the density and the orientational order parameters decay much more rapidly than the translational order parameter. This observation of structural order extending beyond the solid density is in good agreement with the results of density functional theory [6] and prior computer simulations of crystallization in monatomic systems.[7] The translational order parameter at the center of the critical nucleus has almost the same value at all temperatures. By contrast, at small radii the orientational order parameter significantly increases as the supercooling deepens. This result reflects the fact that the solid-state transition to the orientationally well-ordered low-energy phase at 100 K started immediately after the onset of crystallization.

The difference between the profiles for the density and translational order parameters leads, therefore, to ambiguities in the estimation of the sizes of critical nuclei. Following prior convention, if we define the radius of a critical nucleus to be at the position $r_{1/2}$, where the density profile is halfway between its solid and liquid values, the radius would be 5 Å at 100 K and 6 Å at 140 K, corresponding to 5 and 9 molecules, respectively. A similar size for the critical nucleus was also obtained from both the classical nucleation theory and Gránásy's diffuse interface theory. Both of these theories invoke a free energy of freezing per unit volume based on the bulk value, an assignment which, as will be discussed later, cannot be relied upon quantitatively for an aggregate of only a half-dozen molecules. On the other hand, if we choose the radius of a critical nucleus to correspond to the equimolar radius r_e of the density (or orientational order) profile (where the deficit of solidlike molecules inside the dividing surface is balanced by the number of like molecules on the outside), then the critical radius is shifted to 8−8.5 Å and the nucleus contains 20−25 molecules. To compound the uncertainty, if the translational order parameter is chosen to estimate the size of the critical nucleus, our MD results place $r_{1/2}$ at 10 Å and 11 Å, a radius encompassing 40−55 molecules. This result is in rather good agreement with our visual estimates based on fluctuations in the sizes of bulklike aggregates. This is not surprising because we based our original definition of solidlike molecules on the degree of translational order. On the other hand, had the dividing line for the translational order parameter been placed at r_e, it would have encompassed 70−85 molecules. The larger critical nucleus based on the translational order parameter, then, has a core with crystalline density and crystalline molecular orientations surrounded by a less dense layer with translational but not rotational order.

One way to account for the above ambiguity in sizes of critical nuclei and to interpret the profiles of order parameters for freezing is to avail ourselves of Turnbull's hypothesis[34] advanced long before any MD or density functional treatments were carried out. Turnbull pointed out that since nature abhors a vacuum, a naturally disordered liquid in contact with an ordered solid particle will tend to order itself to conform with the surface of the sold. That is the rationale for Turnbull's postulate of a negative excess entropy for the liquid−solid interface. Such a negative interfacial entropy would explain Turnbull's experimental results for mercury, which indicated an *increase* in interfacial free energy as the temperature is increased. Applied to the present situation, this interpretation would identify the ordered region beyond the volume possessing crystalline density with Turnbull's ordered *liquid* at the interface, not with the solid. Therefore, if this interpretation is correct, it is the density profile, not the translational order profile, that best characterizes the solid and identifies n^*, the number of molecules in the critical nucleus.

There is a test of the plausibility of this interpretation. Let us extend the CNT to remedy its most serious failings. We express $\Delta G(r)$, the free energy to form a nucleus of solid in the liquid (for simplicity, ignoring the effect of Laplace pressure and assuming the nucleus to be spherical), as

$$\Delta G = 4\pi r_s^2 \sigma_{sl} + \frac{4}{3}\pi r_e^{\,3} \Delta G_v \tag{23}$$

following the form of the CNT but departing from it in two ways. First we differentiate between the radius of the surface of tension, r_s, and the equimolar radius r_e. Following Tolman, we allow for the possible difference between these radii, defining an interfacial thickness

$$\delta_T = r_e - r_s \tag{24}$$

a thickness not to be confused with the DIT δ. Second, we do not require ΔG_v, the free energy of freezing per unit volume, to be the same for the formation of the nucleus as that for the freezing of the bulk material. Instead, we suppose that ΔG_v for a small aggregate is smaller than that for bulk matter, and we consider it to be a continuous function of the radius of the aggregate increasing from zero at $r = 0$ to its asymptotic value for large r. A variety of one-parameter functions were proposed for ΔG_v (see below), and all gave nominally the same results. We then determine both σ_{sl} and $\Delta G_v(r^*)$ from the nucleation rate combined with our independent estimate of n^* from MD analyses. First, let us neglect the Tolman δ_T, about which very little is known for solid nuclei. From the nucleation rate we get the free energy barrier, ΔG^*, and taking the nucleus to be spherical so that n^* is $4\pi(r^*)^3/3\nu_m$, we adjust the value of both σ_{sl} and the single parameter, a, in $\Delta G_v(a, r)$ to make the maximum of ΔG of eq 24 occur at ΔG^* and r^*. This establishes the two quantities we seek, σ_{sl} and $\Delta G_v(r^*)$.

The six one-parameter functional forms investigated to represent the quantity $f(a,r) \equiv \Delta G_v(a,r)/\Delta G_v(r_\infty)$ were

$$f(a,r) = [r/(a + r)]^m \tag{25}$$

with $m = 1$ or 2 and

$$f(a,r) = 1 - \{\exp[-(r/a)^m]\}^x \tag{26}$$

with $x = 1$, $m = 1$ or 2, and $m = 1$, $x = (r/a)$ or $\exp(r/a)$.

It turns out the critical nuclei identified by our translational order parameter criterion have roughly 6 times as many molecules as that predicted by the standard CNT. It is possible in our simulation that we selected a nucleus that was slightly postcritical and, hence, somewhat too large, but it is highly unlikely that we overestimated by a factor of 6. Taking the ratio n^*/n^*(CNT) to be 6 so that r^* is $6^{1/3}$ times larger than the CNT value, by applying eqs 25 and 26 we find that the "corrected" values of ΔG_v and σ_{sl} are, respectively, 0.07−0.09 and 0.18−0.21 times the CNT values. Such a large correction for ΔG_v seems excessive in view of the close similarities between the core and bulk properties of the SeF_6 clusters found in prior MD simulations.[39] Likewise appearing to be far too large is the correction to the interfacial free energy. The value of 0.014 J/m^2 from the CNT analysis is in fair agreement with the value expected from Turnbull's empirical relation,[40] which has held up well in our studies of transitions in clusters in supersonic flow. For the value to be only 20% of the empirically expected value is dubious. Of course, the empirical relation itself came from an application of the CNT but at such a shallow supercooling (yielding large critical nuclei) that the CNT could be expected to be a more accurate approximation. If we had included the Tolman δ_T correction of eq 24, the discrepancies between the calculated (CNT) and observed (MD translational order) results would have been reduced if δ_T happened to be positive, or worsened if δ_T were to prove negative. Since, to our knowledge, there is no evidence that δ_T is appreciable for solid−liquid interfaces, we ignore its effect in the following.

For the above reasons, the conclusion that our criterion for determining the sizes of critical nuclei from the translational structural order parameter is too inclusive now seems almost inescapable. It recognizes too many molecules as being in the crystalline solid. It identifies the Turnbull-ordered liquid layer of molecules surrounding the nucleus with the solid nucleus itself. Next, we address the problem of where to draw the dividing radius in the density/orientational order parameter profile. Here there is a difference of a factor of perhaps 2 or 3. If we apply the same test based on eqs 25 and 26, we find somewhat more moderate discrepancies between the $r_{1/2}$ and r_e conventions than when we compared results for the density vs the translational order parameters. Therefore, no really clear-cut decision between the two radii can be made from our results on this basis. Despite previous usage, the rational parameter for the density profile is r_e, not $r_{1/2}$. The trouble with this order parameter is its poor sensitivity because of the small difference in density between the liquid and solid phases. For the other order parameters, which in some sense depend on arbitrary criteria, there is less physical reason to discriminate between r_e and $r_{1/2}$. Nevertheless, it is likely that the dividing radius is somewhat larger than $r_{1/2}$. Hence, it is probable that the value of ΔG_v for the critical nucleus is appreciably smaller at r^* than the bulk value assumed to be valid in the CNT and that the σ_{sl} is also somewhat smaller than that derived by applying the CNT. It is clear, however, that the size of critical nuclei inferred from the translational order parameter and from the fluctuations in the number of bulklike solid molecules is much too large. Accordingly, it appears that the results of the MD simulations do not disagree with the classical nucleation theory nearly as severely as we had originally concluded.[29] Moreover, the MD results go a long way toward corroborating Turnbull's negative entropy hypothesis, a hypothesis which has received less attention by current theorists than it would seem to merit.

Acknowledgment. This research was supported by a grant from the National Science Foundation.

References and Notes

(1) Kelton, K. F. *Solid State Phys.* **1991**, *45*, 75.
(2) Laaksonen, A.; Talanquer, V.; Oxtoby, D. W. *Annu. Rev. Phys. Chem.* **1995**, *46*, 489.
(3) Bartell, L. S. In *Theoretical Aspects and Computer Modeling of the Molecular Solid State*; Gavezzotti, A., Ed.; Wiley & Sons: Chichester, 1997.
(4) Chushak, Y.; Bartell, L. S. *J. Phys. Chem.* **1999**, *103*, 11196.
(5) Kashchiev, D.; Sato, K. *J. Chem. Phys.* **1998**, *109*, 8530.
(6) (a) Harrowell, P.; Oxtoby, D. W. *J. Chem. Phys.* **1984**, *80*, 1639. (b) Shen, Y. C.; Oxtoby, D. W. *J. Chem. Phys.* **1996**, *104*, 4233.
(7) ten Wolde, P. R.; Ruiz-Montero, M. J.; Frenkel, D. *J. Chem. Phys.* **1996**, *104*, 9932.
(8) Kolmogorov, A. N. *Bull. Acad. Sci. USSR, Div. Chem. Sci. (Engl. Transl.)* **1937**, *3*, 355.
(9) Johnson, W. A.; Mehl, R. F. *Trans. Am. Inst. Min. Metall. Eng.* **1939**, *135*, 416.
(10) Avrami, M. *J. Chem. Phys.* **1939**, *7*, 1103; **1940**, *8*, 212; **1941**, *9*, 177.
(11) Markworth, A. J. *Mater. Sci. Eng.* **1988**, *100*, 169.
(12) Weinberg, M. C. *J. Non-Cryst. Solids* **1991**, *134*, 116; **1992**, *142*, 126.
(13) Levine, L. E.; Lakshmi Narayan, K.; Kelton, K. F. *J. Mater. Res.* **1997**, *12*, 124.
(14) Kinney, K. E.; Xu, S.; Bartell, L. S. *J. Phys. Chem.* **1996**, *100*, 6935.
(15) Powell, B. M.; Dolling, G. *Can. J. Chem.* **1988**, *66*, 897.
(16) Tanemura, M.; Hiwatari, Y.; Matsuda, H.; Ogawa, T.; Ogita, N.; Ueda, A. *Prog. Theor. Phys.* **1977**, *58*, 1079.
(17) Steinhardt, P. J.; Nelson, D. R.; Ronchetti, M. *Phys. Rev. B* **1983**, *28*, 784.
(18) Mountain, R. D.; Brown, A. C. *J. Chem. Phys.* **1984**, *80*, 2730.
(19) van Duijneveldt, J. S.; Frenkel, D. *J. Chem. Phys.* **1992**, *96*, 4655.
(20) Gutzow, I.; Kashchiev, D. In *Advances in Nucleation and Crystallization of Glasses*; Hench, L. L., Freiman, S. W., Eds.; American Ceramic Society: Westerville, OH, 1971.
(21) Shi, G.; Seinfeld, J. H. *J. Mater. Res.* **1991**, *6*, 2091.
(22) Shneidman, V. A.; Weinberg, M. C. *J. Non-Cryst. Solids* **1993**, *160*, 89.
(23) Dobreva, A.; Stoyanov, S.; Tzuparska, T.; Gutzow, I. *Thermochim. Acta* **1996**, *280-281*, 127.
(24) Ostwald, W. *Z. Phys. Chem., Stoechiom. Verwandtschaftsl.* **1897**, *22*, 289.
(25) Kelton, K. F.; Greer, A. L. *J. Non-Cryst. Solids* **1986**, *79*, 295.
(26) Pawley, G. S.; Thomas, G. W. *Phys. Rev. Lett.* **1982**, *48*, 410. Pawley, G. S.; Dove, M. T. *Chem. Phys. Lett.* **1983**, *99*, 45.
(27) Fuchs, A. H.; Pawley, G. S. *J. Phys. (Paris)* **1988**, *49*, 41.
(28) Chushak, Y.; Santikary, P.; Bartell, L. S. *J. Phys. Chem.* **1999**, *103*, 5636.
(29) Bartell, L. S.; Dibble, T. S. *J. Phys. Chem.* **1991**, *95*, 1159.
(30) Turnbull, D.; Fisher, J. C. *J. Chem. Phys.* **1949**, *17*, 71.
(31) Turnbull, D. *J. Chem. Phys.* **1952**, *20*, 411.
(32) Santikary, P.; Kinney, K. E.; Bartell, L. S. *J. Phys. Chem.* **1998**, *102*, 10324.
(33) Granasy, L. *J. Non-Cryst. Solids* **1994**, *162*, 301. Granasy, L. *Mater. Sci. Eng.* **1994**, *A178*, 121. Granasy, L. *J. Phys. Chem.* **1995**, *99*, 14183.
(34) Turnbull, D. In *Physics of Non-Crystalline Solids*; Prins, J. A., Ed.; North-Holland: Amsterdam, 1964; p 4.
(35) Bartell, L. S.; Xu, S. *J. Phys. Chem.* **1995**, *96*, 10446.
(36) Turnbull, D. *J. Appl. Phys.* **1950**, *21*, 1022.